Antimicrobial Rubrolides from a South African Species of *Synoicum* Tunicate

Justyna Sikorska[†], **Shirley Parker-Nance**[†], **Michael T. Davies-Coleman**[†], **Oliver B. Vining**[†], **Aleksandra E. Sikora**[†], and **Kerry L. McPhail**[*,†]

[†]Department of Pharmaceutical Sciences, College of Pharmacy, 203 Pharmacy Building, Oregon State University, Corvallis, Oregon 97331, United States

[‡]Centre for African Conservation Ecology, Department of Zoology, Nelson Mandela Metropolitan University, PO Box 77000, Port Elizabeth 6031, South Africa, Faculty of Natural Sciences

[§]University of the Western Cape, Private Bag X17, Belville 7535, South Africa

Abstract

The CH_2Cl_2-MeOH extract of a South African tunicate described as the new *Synoicum globosum* Parker-Nance sp. nov. (Ascidiacea, Aplousobranchia) was subjected to ^{1}H NMR-guided fractionation. This resulted in the identification of new 3″-bromorubrolide F (**1**), 3′-bromorubrolide E (**2**), 3′-bromorubrolide F (**3**) and 3′, 3″-dibromorubrolide E (**4**), and reisolation of known rubrolides E (**5**) and F (**6**), based on NMR spectroscopic and mass spectrometric data. Biological testing of both new and known members of this reported antimicrobial family of halogenated, aryl-substituted furanones indicated moderate antibacterial properties for 3′-bromorubrolide E (**2**), 3′, 3″-dibromorubrolide E (**4**), and rubrolide F (**6**) against methicillin-resistant *Staphylococcus aureus* (MRSA) and *S. epidermidis*.

Marine organisms have proven to be a rich source of new chemical entities, and the first marine drugs have been approved, with others continuing in clinical trials.[1,2] In particular, ascidians (tunicates) have provided a variety of clinical candidates and new carbon skeletons including non-nitrogenated, halogenated rubrolides, the first of which were isolated from British Columbian specimens of the ascidian *Ritterella rubra*.[3] Rubrolides comprise a central furanone ring substituted at C-4 and C-5 with phenolic moieties. The phenolic moieties are differentially halogenated in the known rubrolides A-O. However, among them only rubrolide F is selectively methylated at C-4″.[3-5] Attempts to synthesize new, more potent antimicrobials resulted in a suite of analogues having one or two phenolic moieties with varying halogenation and hydroxy group methylation.[6,7] The biological activities of the known rubrolide natural products and their synthetic analogues include antibacterial activity against *Staph. aureus* and *Bacillus subtilis* (rubrolides A, B, C),[3] selective inhibition of protein phosphatases 1 and 2A,[3] weak to moderate activity against various cancer cell lines (rubrolides I, K, L, M),[4] inhibition of human aldose reductase (rubrolide L),[8,9] and moderate anti-inflammatory properties (rubrolide O).[10] Interestingly, a synthetic series of analogues in which the furanone is substituted with an aryl group comprises potent inhibitors of bacterial

cell wall biosynthesis, which have been patented for their potential antimicrobial applications.[11]

As part of our ongoing investigation of a 2004 collection of organic extracts from South African ascidians,[12] ^{1}H NMR and MS screening identified a *Synoicum* CH_2Cl_2-MeOH extract that exhibited a complex aromatic ^{1}H signature as well as isotopic patterns for halogenated mass ions. Successive fractionation of this extract (2.4 g) by RP SPE followed by RP HPLC yielded four new rubrolide analogues (**1-4**) together with the known rubrolides E (**5**) and F (**6**).
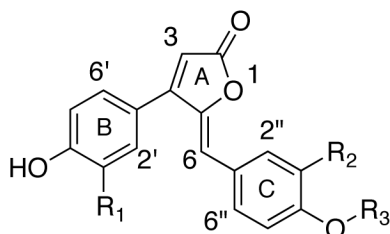
1	R_1 = H, R_2 = Br, R_3 = Me
2	R_1 = Br, R_2 = H, R_3 = H
3	R_1 = Br, R_2 = H, R_3 = Me
4	R_1 = Br, R_2 = Br, R_3 = H
5	R_1 = H, R_2 = H, R_3 = H
6	R_1 = H, R_2 = H, R_3 = Me

A molecular formula of $C_{18}H_{13}O_4Br$ for rubrolide **1** was deduced from the HRESIMS ion cluster for $[M+H]^+$ at *m/z* 373.0081/375.0070 (1:1). Inspection of the ^{1}H NMR spectrum revealed nine olefinic or aromatic signals (δ_H 6.23 – 8.10, Table 1) and a 3H midfield singlet consistent with an aromatic *O*-methyl (δ_H 3.93) group. Multiplicity-edited HSQC and HMBC data indicated the presence of eight quaternary carbons (δ_C 120.5, 126.5, 133.5, 146.7, 156.9, 159.4, 159.9, 169.5), nine methine carbons (δ_C 111.1, 111.6, 111.7, 115.6, 115.6, 129.9, 129.9, 131.2, 134.6) and one *O*-methyl carbon (δ_C 55.3). HMBC correlations from a ^{1}H doublet at δ 6.23 (H-3) to ^{13}C resonances at δ 169.5 (C-2), 159.4 (C-4) and 146.7 (C-5) defined the furanone (ring A) of the rubrolide skeleton. A *para*-substituted phenolic moiety was indicated by two mutually coupled 2H doublets (δ_H 7.47 and 6.95), and confirmed by apparent HMBC correlations from these doublets to their same HSQC-correlated ^{13}C resonances. This B-ring could be located at C-4 of ring A based on an HMBC correlation from the H-2′/6′ doublet (δ_H 7.47) to the C-4 resonance. The presence of COSY couplings between H-5″ and H-6″ ^{1}H signals, in parallel with a long range coupling (2.1 Hz) between H-2″ and H-6″, led to assignment of ring C as a 1, 3, 4-trisubstitued aromatic moiety. Inspection of the HMBC data for **1** to establish the connectivity between rings A and C identified the olefinic linkage H-6 (δ_H 6.28, s). HMBC correlations were observed from the H-6 singlet to ^{13}C resonances for C-4 and C-5 of ring A, and to C-2″ and C-6″ of ring C. Deshielded methoxy H$_3$-7″ showed an HMBC correlation to C-4″, thus locating this substituent on ring C. A relatively shielded quaternary carbon resonance at δ_C 126.5, assigned as C-3″ (from HMBC correlations) in the 1, 3, 4-trisubstituted ring C, remained as the site of bromine substitution. Therefore, rubrolide **1** was assigned as 5-(3-bromo-4-methoxybenzylidene)-4-(4-hydroxyphenyl)furan-2(5*H*)-one, and given the trivial name 3″-bromorubrolide F.

HRESIMS of rubrolide **2** gave an [M+H]$^+$ ion cluster at *m/z* 358.9933/360.9916 (1:1) for a molecular formula of $C_{17}H_{11}O_4Br$. Comparison of the ^{1}H NMR spectra for **1** and **2** indicated significant changes in the shifts for all downfield ^{1}H signals and the absence of the midfield 3H singlet (δ 3.93, Table 1). Assignment of COSY and HMBC correlations showed that in the case of **2**, ring B is the 1, 3, 4-trisubstitued aromatic moiety, and ring C is the 1,4-disubstitued aromatic unit. Therefore, it could be concluded that in **2**, the bromine is located at C-3′ of ring B. The lack of an *O*-methyl singlet indicated a free 4″-hydroxy group in **2** compared to **1**. Thus, the structure of **2** was defined as 4-(3-bromo-4-hydroxyphenyl)-5-(4-hydroxybenzylidene)furan-2(5*H*)-one, and given the trivial name 3′-bromorubrolide E.

The HRESIMS data for rubrolide **3** gave an [M+H]$^+$ ion cluster at *m/z* 373.0060/375.0048 (1:1), for the same molecular formula of $C_{18}H_{13}O_4Br$ as that for **1**. Comparison of the ^{1}H chemical shifts for **2** and **3** showed a slight upfield shift for B-ring ^{1}H resonances (H-2′, H-5′ and H-6′) and a large downfield shift for C-ring ^{1}H resonances (H-2″, H-3″, H-5″ and H-6″, Table 1). The larger variations in δ$_H$ values for ring C could be explained by methylation of OH-4″ in **3**, as confirmed by an HMBC correlation from a 3H singlet at δ 3.84 (H$_3$-7″) to the C-4″ resonance (δ$_C$ 162.1). Therefore, the structure of rubrolide **3** was assigned as 4-(3-bromo-4-hydroxyphenyl)-5-(4-methoxybenzylidene)furan-2(5*H*)-one, and given the trivial name 3′-bromorubrolide F.

Rubrolide **4** has a molecular formula of $C_{17}H_{10}O_4Br_2$ as assigned from the [M−H]$^-$ ion cluster at *m/z* 434.8873/436.8929/438.8940 (1:2:1). Examination of the ^{1}H and COSY NMR data indicated that the ^{1}H shifts for ring B protons (H-2′, H-5′ and H-6′) were similar to those for ring B of 3′-bromorubrolide E (**2**, Table 1). Additionally, COSY-coupled H-2″/H-6″ and H-5″/H-6″ established ring C as a 1, 3, 4-trisubstitued benzene. The assignment of quaternary C-3′ (δ$_C$ 113.1) and C-3″ (δ$_C$ 112.7), as deduced from HMBC, localized bromine substituents at these positions. Thus, rubrolide **4** was assigned as 5-(3-bromo-4-hydroxybenzylidene)-4-(3-bromo-4-hydroxyphenyl)furan-2(5*H*)-one, and given the trivial name 3′,3″-dibromorubrolide E.

For new rubrolides **1**-**4**, determination of the C-5/C-6 double bond geometry relied on NOE data. NOEs between H-6 and both H-2′/H-6′ and H-2″/H-6″ (where one of the pair was always distinguishable) were observed, placing H-6 in close proximity to both phenyl rings and concluding a Z geometry of the exocyclic double bond.[10]

The HRESIMS data for compounds **5** and **6** suggested their identities as rubrolides E and F, respectively. 1D and 2D NMR data were acquired in methanol-*d$_4$* for compound **5**, and readily confirmed its identity as rubrolide E, although previously reported data were acquired in CDCl$_3$ and DMSO-*d$_6$*.[3] The initially acquired NMR data in methanol-*d$_4$* for compound **6** were consistent with previously published ^{1}H NMR data for rubrolide F.[3] However, after additional purification of compound **6**, significant changes in ^{1}H shifts for the A and B rings were observed, while 2D NMR data provided the same rubrolide F structure as initially assigned. One explanation for this observation was the interconversion of **6** between phenoxy and phenol forms. The addition of NaOH to the NMR tube containing **6** caused a shift in ring A and B ^{1}H resonances, which was reversed after the addition of formic acid (Figures S25-27). Although the addition of NaOH did not reproduce the exact chemical shifts previously reported,[3] or observed for the initially isolated natural product here, it could be concluded that rubrolide F was first isolated as a salt (other than Na$^+$) of the phenoxy (B-ring) anion in both cases. Our subsequent re-purification performed under neutral conditions resulted in protonation to yield the phenol form of **6** (Table S6).

Finally, we tested in vitro activities of rubrolides **1**-**4** as well as **5** and **6** against a panel of pathogenic bacteria including MRSA, *S. epidermidis*, gentamycin and vancomycin resistant

Enterococcus faecalis and *Escherichia coli*, (Table 2). Overall, 3′-bromo-rubrolide F (**3**) and rubrolide F (**6**) showed significantly higher IC_{50} values and a lower percentage of growth inhibition than their non-methylated analogues. This trend was previously observed for synthetic rubrolide analogues tested against NCI-H460, MCF-7 and SF-268 cell lines,[7] and may indicate a differential cell permeability.

EXPERIMENTAL SECTION

General Experimental Procedures

UV spectra were acquired on a JASCO J-815 CD spectrometer. NMR data were acquired in methanol-d_4 referenced to residual CH_3OH chemical shifts (δ_C 49.2, δ_H 3.31) on a Bruker Avance III 700 MHz spectrometer equipped with a 5mm ^{13}C cryogenic probe. HRESIMS data were acquired in positive mode on a Waters Micromass LCT Premier and AB SCIEX Triple TOF 5600. HPLC purifications were performed using a Shimadzu dual LC-20AD solvent delivery system with a Shimadzu SPD-M20A UV/VIS photodiode array detector.

Ascidian Collection

Synoicum globosum Parker-Nance sp. nov. was collected on July 20, 2004 by hand using SCUBA at a depth of 18 m in the White Sands Reef in Algoa Bay, Eastern Cape Province, South Africa (33:59.916S, 25:42.573W). The type specimen (SAF2004-54) for this new ascidian species is housed at the South African Institute for Aquatic Biodiversity (SAIAB), Grahamstown, South Africa.

Ascidian Taxonomy

A descriptive synopsis of the new species *Synoicum globosum* Parker-Nance sp. nov. (Ascidiacea, Aplousobranchia) relative to known congeners and a detailed morphological description with figures are provided in the Supporting Information. In summary, colonies are gelatinous but firm and consist of egg-shaped heads on a short cone-shaped stalk with irregular basal mass. Externally, the surface of the head is free of sand, although a dense accumulation of fine sand particles is visible in the surface layer of the stalk and the wider irregular basal attachment mass is heavily encrusted with larger sand particles and epifauna. Zooids are red and arranged in circular systems clearly distinguishable against the mustard yellow test material of freshly collected material. The internal test is transparent with fine sand, shell pieces, as well as other foreign material that decreases in density towards the central part of the colony. The slender zooids (8-20 mm) are closely packed together in a distinct layer, and comprise a thorax (1.0-2.7 mm), abdomen (0.9-2.0 mm) and posterior abdomen (6.0-14.8 mm). The branchial opening has six small lobes and the atrial opening is small with a single ribbonlike tongue with small distal teeth. The branchial sac has 11-14 rows of stigmata with 10-11 stigmata in each of the rows. One to two larvae are present in developmental sequence in the atrial cavity. Mature larvae (trunk 0.56-0.66 mm in length and 0.14-0.40 mm in width) have 12 or more lateral ampullae arranged in 2-3 rows with epidermal vesicles present dorsally and ventrally and tail wound about halfway around the trunk.

Extraction and Isolation

The organism was extracted with CH_2Cl_2-MeOH 2:1 to yield 1.62 g of organic extract that was subjected to reversed phased solid phase extraction (RP_{18}-SPE) using a stepped gradient of 50-100% MeOH in H_2O. The 75% MeOH-H_2O and 100% MeOH fractions were subsequently separated by RP_{18}-HPLC (Synergi Fusion-RP, Phenomenex, 250 mm × 10 mm, 65 % MeOH-H_2O) to yield 3″-bromorubrolide F (**1**, 3.0 mg), 3′-bromorubrolide E (**2**,

7.4 mg), 3′-bromo-rubrolide F (**3**, 2.8 mg) and 3′, 3″-dibromorubrolide E (**4**, 1.4 mg), rubrolide E (**5**, 13.5 mg) and rubrolide F (**6**, 4.3 mg).

Antibacterial Assay

Antibacterial activity was determined using the microtiter dilution method in a 96 well plate format.[13] Crude extracts were tested at 125, 12.5, and 1.25 µg/mL against a panel of clinically relevant human pathogens including methicillin-resistant *Staphylococcus aureus* (ATCC® BAA-1720[TM]), *S. epidermidis* (ATCC® 35984™), gentamycin and vancomycin resistant *Enterococcus faecalis* (ATCC® 700802™), and *Escherichia coli* (O157:H7)[14] to determine the appropriate concentration range for testing of pure rubrolides. Bacterial strains were cultured as follows: MRSA and *S. epidermidis* in tryptic soy broth (Becton, Dickinson and Co.), *E. faecalis* in brain heart infusion medium (Becton, Dickinson and Co.), and all Gramnegative bacteria in Luria-Bertani liquid medium (Becton, Dickinson and Co). For all experiments, the cultures were inoculated with 5×10^5 cfu/mL in a final volume of 200 µL in 96-well tissue culture treated microtiter plates (Greiner Bio-One) and incubated without shaking at 37 °C for 16 h, at which point bacterial growth was determined turbidimetrically (OD_{600}) using a BioTek Synergy HT multimode plate reader. Each microtiter plate contained a positive control (chloramphenicol at a final concentration of 30 µg/mL), a negative control (bacteria grown in the presence of DMSO), and a contamination control (medium only). IC_{50} values for rubrolides **1**-**6** were determined against MRSA and *S. epidermidis* as described above, using a concentration range of 130 - 0.3 µg/mL. Additionally, the susceptibility of *E. faecalis* and *E. coli* to pure compounds was tested at 100 µg/mL. Test samples were inoculated in technical duplicate on each plate and assays were performed in biological triplicate. Percentage growth inhibition was determined using the plate-based microtiter dilution assay, and IC_{50} values were derived using nonlinear regression analysis.

3″-Bromorubrolide F (1)—Yellow amorphous solid; UV (MeOH) λ_{max} (log ε) 248 (3.8), 356 (4.0) nm; HRESIMS [M+H]⁺ (50%) *m/z* 373.0081, (calcd for $C_{18}H_{14}O_4{}^{79}Br$, 373.0075), [M+H]⁺ (50%) *m/z* 375.0070, (calcd for $C_{18}H_{14}O_4{}^{81}Br$, 375.0055); ¹H and ¹³C NMR data (Table 1); COSY, HMBC, NOESY data (Table S1).

3′-Bromorubrolide E (2)—Yellow amorphous solid; UV (MeOH) λ_{max} (log ε) 250 (4.1), 371 (4.3) nm; HRESIMS [M+H]⁺ (50%) *m/z* 358.9933, (calcd for $C_{17}H_{12}O_4{}^{79}Br$, 358.9919), [M+H]⁺ (50%) *m/z* 360.9916, (calcd for $C_{17}H_{12}O_4{}^{81}Br$, 360.9899); ¹H and ¹³C NMR data (Table 1); COSY, HMBC, NOESY data (Table S2).

3′-Bromorubrolide F (3)—Yellow amorphous solid; UV (MeOH) λ_{max} (log ε) 248 (3.8), 365 (3.9) nm; HRESIMS [M+H]⁺ (50%) *m/z* 373.0060, (calcd for $C_{18}H_{14}O_4{}^{79}Br$, 373.0051), [M+H]⁺ (50%) *m/z* 375.0048, (calcd for $C_{18}H_{14}O_4{}^{81}Br$, 375.0055); ¹H and ¹³C NMR data (Table 1); COSY, HMBC, NOESY data (Table S3).

3′, 3″-Dibromorubrolide E (4)—Yellow amorphous solid; UV (MeOH) λ_{max} (log ε) 254 (4.0), 366 (4.1), 444 (3.6) nm; HRESIMS [M–H]⁻ (25%) *m/z* 434.8872, (calcd for $C_{17}H_9O_4{}^{79}Br{}^{81}Br$, 434.8868), [M–H]⁻ (50%) *m/z* 436.8853, (calcd for $C_{17}H_9O_4{}^{79}Br{}^{81}Br$, 436.8847), [M–H]⁻ (25%) *m/z* 438.8835, (calcd for $C_{17}H_9O_4{}^{81}Br_2$, 438.8827); ¹H and ¹³C NMR data (Table 1); COSY, HMBC, NOESY data (Table S4).

Rubrolide E (5)—Yellow amorphous solid; UV (MeOH) λ_{max} (log ε) 226 (3.9), 247 (3.9), 368 (4.0) nm; HRESIMS [M+H]⁺ *m/z* 281.0821, (calcd for $C_{17}H_{13}O_4$, 281.0814); ¹H NMR (400 MHz, CD₃OD) 7.69 (2H, d, *J* = 8.8 Hz, H-2″, H-6″), 7.44 (2H, d, *J* = 8.6 Hz, H-2′, H-6′), 6.91 (2H, d, *J* = 8.5 Hz, H-3′, H-5′) 6.81 (2H, d, *J* = 8.8 Hz, H-2″, H-6″), 6.30 (1H,

s, H-5), 6.11 (1H, s, H-2); ^{13}C NMR (100 MHz, methanol-d_4) 171.5 (C, C-1), 161.0 (C, C-3), 159.7 (C, C-4′, C-4″), 145.0 (C, C-4), 133.7 (CH, C-2″, C-6″), 131.2 (CH, C-2′, C-6′), 126.5 (CH, C-3″, C-5″), 125.0 (C, C-1″), 120.6 (C, C-1′), 117.2 (CH, C-3′, C-5′), 115.9 (CH, C-5), 110.7 (CH, C-2), see Table S5 for 2D data and literature for CDCl$_3$[15] and DMSO-d_6^3 NMR data.

Rubrolide F (6)—Yellow amorphous solid; UV (MeOH) λ_{max} (log ε) 248 (3.8), 356 (4.0) nm; HRESIMS [M+H]$^+$ m/z 295.0985, (calcd for C$_{18}$H$_{15}$O$_4$, 295.0970); ^{1}H and ^{13}C NMR data (Table S6).

Supplementary Material

Refer to Web version on PubMed Central for supplementary material.

Acknowledgments

REFERENCES

(1). Kong D-X, Jiang Y-Y, Zhang H-Y. Drug Discov. Today. 2010; 15:884–886. [PubMed: 20869461]

(2). Montaser R, Luesch H. Future Med. Chem. 2011; 3:1475–1489. [PubMed: 21882941]

(3). Miao S, Andersen RJ. J. Org. Chem. 1991; 56:6275–6280.

(4). Ortega MJ, Zubía E, Ocaña JM, Naranjo S, Salvá J. Tetrahedron. 2000; 56:3963–3967.

(5). Pearce AN, Chia EW, Berridge MV, Maas EW, Page MJ, Webb VL, Harper JL, Copp BR. J. Nat. Prod. 2006; 70:111–113. [PubMed: 17253860]

(6). Bellina F, Anselmi C, Viel S, Mannina L, Rossi R. Tetrahedron. 2001; 57:9997–10007.

(7). Bellina F, Anselmi C, Martina F, Rossi R. Eur. J. Org. Chem. 2003; 12:2290–2302.

(8). Manzanaro S, Salvá J, de la Fuente JÁ. J. Nat. Prod. 2006; 69:1485–1487. [PubMed: 17067167]

(9). Boukouvalas J, McCann LC. Tetrahedron Lett. 2010; 51:4636–4639.

(10). Pearce AN, Chia EW, Berridge MV, Maas EW, Page MJ, Webb VL, Harper JL, Copp BR. J. Nat. Prod. 2006; 70:111–113. [PubMed: 17253860]

(11). Caufield, CE.; Antane, SA.; Morris, KM.; Naughton, SM.; Quagliato, DA.; Andrae, PM.; Enos, A.; Chiarello, JF. A61K 31/341. Office, USP., editor. Wyeth, Madison, NJ (US): USA: 2009. p. 35

(12). Sikorska J, Hau AM, Anklin C, Parker-Nance S, Davies-Coleman MT, Ishmael JE, McPhail KL. J. Org. Chem. 2012; 77:6066–6075. [PubMed: 22712890]

(13). Smith SM, Beattie AJ, Gillings MR, Holley MP, Stow AJ, Turnbull CL, Wilson PD, Briscoe DA. J. Microbiol. Methods. 2008; 72:103–106. [PubMed: 18054097]

(14). Sikora AE, Beyhan S, Bagdasarian M, Yildiz FH, Sandkvist M. J. Bacteriol. 2009; 191:5398–5408. [PubMed: 19542276]

(15). Tale NP, Shelke AV, Tiwari GB, Thorat PB, Karade NN. Helv. Chim. Acta. 2012; 95:852–857.

Table 1

¹H (700 MHz) and ¹³C (175 MHz) NMR Spectroscopic Data (methanol-d_4) for Rubrolides **1-4**.

position	3″-Bromorubrolide F (1)		3′-Bromorubrolide E (2)		3′-Bromorubrolide F (3)		3′,3″-Dibromorubrolide E (4)	
	δ_C, mult.	δ_H (mult., J in Hz)	δ_C, mult.	δ_H (mult., J in Hz)	δ_C, mult.	δ_H (mult., J in Hz)	δ_C, mult.	δ_H (mult., J in Hz)
2	169.5 (C)		170.4 (C)		171.5 (C)		171.5 (C)	
3	111.1 (CH)	6.23 (d, 0.6)	111.9 (CH)	6.20 (s)	111.4 (CH)	6.16 (s)	111.7 (CH)	6.16 (s)
4	159.4 (C)		158.3 (C)		159.5 (C)		159.5 (C)	
5	146.7 (C)		146.3 (C)		147.8 (C)		147.5 (C)	
6	111.6 (CH)	6.28 (s)	114.5 (CH)	6.24 (s)	115.0 (CH)	6.31 (s)	114.7 (CH)	6.22 (s)
1′	120.5 (C)		123.2 (C)		121.3 (C)		122.3 (C)	
2′	129.9 (CH)	7.47 (d, 8.6)	133.6 (CH)	7.72 (d, 2.0)	134.1 (CH)	7.70 (d, 2.2)	134.4 (CH)	7.70 (d, 2.2)
3′	115.6 (CH)	6.95 (d, 8.7)	110.9 (C)		113.3 (C)		113.1 (C)	
4′	159.9 (C)		157.4 (C)		161.6 (C)		161.2 (C)	
5′	115.6 (CH)	6.95 (d, 8.7)	116.8 (CH)	7.03 (d, 8.3)	118.9 (CH)	6.94 (d, 8.3)	118.8 (C)	6.97 (d, 8.4)
6′	129.9 (CH)	7.47 (d, 8.6)	129.5 (CH)	7.42 (dd, 8.3, 2.0)	130.2 (CH)	7.38 (dd, 8.3, 2.2)	130.5 (CH)	7.39 (d, 8.4, 2.2)
1″	133.5 (C)		125.2 (C)		127.4 (C)		126.3 (C)	
2″	134.6 (CH)	8.10 (d, 2.1)	133.2 (CH)	7.70 (d, 8.7)	133.5 (CH)	7.79 (d, 8.6)	136.7 (CH)	8.03 (d, 2.1)
3″	126.5 (C)		116.0 (CH)	6.83 (d, 8.7)	115.2 (CH)	6.98 (d, 8.9)	112.7 (C)	
4″	156.9 (C)		159.6 (C)		162.1 (C)		159.6 (C)	
5″	111.7 (CH)	7.10 (d, 8.6)	116.0 (CH)	6.83 (d, 8.7)	115.2 (CH)	6.98 (d, 8.9)	118.3 (CH)	6.87 (d, 8.6)
6″	131.2 (CH)	7.78 (dd, 8.6, 2.1)	133.2 (CH)	7.70 (d, 8.7)	133.5 (CH)	7.79 (d, 8.6)	132.9 (CH)	7.59 (dd, 8.6, 2.1)
7″	55.3 (CH₃)	3.93 (s)			55.8 (CH₃)	3.84 (s)		

Table 2

Antibacterial Properties of Rubrolides **1-6**.

Compound	MRSA	*S. epidermidis*	*E. faecalis*	*E. coli*
	^{a}IC$_{50}$ μM (SEM)	^{a}IC$_{50}$ μM (SEM)	Percent growth inhibition at 100 μg/mL (SEM)	
3″-Bromorubrolide F (**1**)	256 (1.3)	98 (1.2)	43 (8.3)	22 (1.9)
3′-Bromorubrolide E (**2**)	82 (1.4)	38 (1.7)	16 (14.1)	0 (26.2)
3′-Bromorubrolide F (**3**)	360 (1.3)	42 (1.2)	2 (3.1)	14 (14.4)
3′, 3″-Dibromorubrolide E (**4**)	89 (1.3)	28 (1.4)	2 (12.9)	25 (4.6)
Rubrolide E (**5**)	105 (1.5)	21 (1.5)	89 (3.6)	16 (2.8)
Rubrolide F (**6**)	1006 (1.3)	79 (1.1)	47 (10.4)	15 (5.5)

^{a}IC$_{50}$ values represent the mean of 3 independent experiments, derived using nonlinear regression analysis; SEM = standard error of the mean